Electronic Supplementary Material (ESI) for Chemical Communications

Synthesis and Characterization of Functional Multicomponent Nanosized Gallium Chelated Gold Crystals

Ajit Zambre,[a‡] Francisco Silva,[b‡] Anandhi Upendran,[c] Zahra Afrasiabi,[d] Yan Xin,[e] António Paulo,[b] and Raghuraman Kannan[a,f,g]*

[a]Departments of [a]Radiology, [c]Physics and [f]Bioengineering, [g]International Center for Nano/Micro Systems and Nanotechnology, University of Missouri-Columbia, Columbia, Missouri-65212. USA;
Tel: 0015738825676; E-mail: kannanr@health.missouri.edu
[b]Centro de Ciências e Tecnologias Nucleares, Instituto Superior Técnico, Estrada Nacional 10 (Km 139,7), 2695-066 Bobadela LRS, Portugal.
[d]Department of Life and Physical Sciences, Lincoln University, Jefferson City, Missouri 65101, USA
[e]National High Magnetic Field Laboratory, Florida State University, Tallahassee, FL 32310, USA
[‡]These authors contributed equally.

Table of Contents

Scheme, Figures, Tables and Video Clip

SUPPORTING INFORMATION

1. Experimental Section

General Information

The materials used for synthesis of gold nanoparticle (AuNPs) were procured from standard vendors. Tetrachloroauric acid trihydrate ($HAuCl_4$. $3H_2O$), sodium borohydride ($NaBH_4$), diethylenetriaminepentacetic acid (DTPA), acetic anhydride, anhydrous pyridine, 2-aminoethanethiol hydrochloride, triethylamine, glacial acetic acid (CH_3COOH), Gallium nitrate ($Ga(NO_3)_3$), sodium hydroxide (NaOH), hydrocloric acid (HCl), methanol (MeOH), diethyl ether (Et_2O), sodium chloride (NaCl), dimethyl formamide (DMF), dimethyl sulfoxide (DMSO), histidine, human serum albumin (HSA), bovine serum albumin (BSA), and cysteine were purchased from Aldrich and used as received. For the preparation of aqueous solutions and for rinsing of gold nanoparticles, Milli-Q (DI) water (ρ>18MΩ) was used. Synthesis of **1** was performed by previously reported protocol.[1, 2] MTT Cell Proliferation Assay kit was obtained from Promega Corporation, USA.

Analytical Measurements

Electron Microscopy: Transmission electron microscope images were obtained on a JEOL 1400 transmission electron microscope (TEM), JEOL LTD., Tokyo, Japan. TEM samples were prepared by placing 5 µL of gold nanoparticle solution on the 300 mesh carbon coated copper grid and the solution allowed to sit five minutes. Excess solution was removed carefully and the grid was allowed to dry an additional five minutes. The average size and size distribution of nanoparticles were determined by processing the TEM image Adobe Photoshop (with Fovea plug-ins). Elements present in **1** and **2** were quantified by energy dispersive spectrometer (EDS) using FEI Quanta 600 FEG Extended Vacuum Scanning Electron Microscope (ESEM). HR-TEM, High angle annular dark field (HAADF), Scanning Transmission Electron Microscopy (STEM) images were obtained on a FEI Tecnai F30 G2 Twin Microscope (300kV), Hillsboro, Oregon 97124 USA. HR-TEM sample grid was prepared on a copper grid (Cu-400HD, Pacific Grid Tech, CA, USA), 400 mesh, 3.05mm O.D., hole size: ~42um, coated with pure carbon holey film and continue carbon film, (~15nm each film). The solution of nanoparticles was dropped on the carbon film and allowed to dry. The grid was immersed in acetone for overnight and dried in an oven at 50-60°C for 30 mins. Electron Energy Loss Spectroscopy (EELS) was performed in a probe corrected JEM-ARM200cF at 200kV.

Dynamic Light Scattering (DLS) Analysis: DLS measurements were performed with a Malvern Zetasizer Nano ZS (Malvern Instruments Ltd. USA) equipped with a 633-nm He-Ne laser and operating at an angle of 173°. The software used to collect and analyze the data was the Dispersion Technology Software version 5.10 from Malvern. 600 µl of each sample was measured in low volume semi-micro disposable sizing cuvettes (Fisher Scientific, USA) with a path length of 10 mm. The measurements were made at a position of 4.65 mm from the cuvette wall with an automatic attenuator. For each sample, 15 runs of 10 seconds were performed, with three repetitions for all the samples. The intensity size distribution, the Z-average diameter (Z-ave) and the polydispersity index (PDI) were obtained from the autocorrelation function using the "general purpose mode" for all nanoparticle samples. The default filter factor of 50% and the default lower threshold of 0.05 and upper threshold of 0.01 were used. Zeta potential measurements were obtained in triplicate using water as dispersant and Huckel model. For each sample, 20 runs were performed with auto analysis mode.

Nanoparticle Tracking Analysis: The hydrodynamic diameters of AuNPs were measured using NanoSight LM10-HSGFT system configured with a temperature controlled LM14G sample viewing unit equipped with a 532 nm (green) laser (NanoSight Limited, Amesbury, UK). Video tracking of the AuNPs based on Raleigh scattering was captured with a monochrome Marlin CCD camera (Allied Vision Technologies, Germany). A 1 mL syringe (Becton Dickinson, NJ) was used to deliver the samples to the viewing chamber and the temperature was held constant at 22ºC. NanoSight 2.2 program was used to collect and analyze sample data. Each size measurement was based on a 30 second video and the Stokes–Einstein equation was used to calculate the mean hydrodynamic diameter. As noted below, the samples were diluted 30-fold relative to the stock AuNP concentration prior to NTA measurements. This dilution was selected such that ~900 particles were tracked in a 30 second video. These conditions provided a representative sampling of the entire sample and are confirmed by the fact that size distribution did not change with longer videos in which significantly more nanoparticles were analyzed. Three measurements were conducted for each sample to provide an average size and standard deviation.

UV-Visible Spectroscopy: The UV-visible absorption spectra were recorded at room temperature using Varian Cary 50 UV/Vis spectrophotometers. The absorption measurements were performed on dilute colloidal gold nanoparticle solution in disposable cuvettes with a 10 mm path length.

ICP-OES Measurements: All measurements were performed in triplicates on Varian Vista – Pro CCD simultaneous inductively coupled plasma – optical emission spectrometer (ICP–OES) (Varian Inc., California, USA) with following parameter: Power (kW) : 1.20; Plasma flow (L/min) : 15.0; Auxiliary flow (L/min) : 1.50; Nebulizer flow (L/min): 0.75; Replicate read time

(s) : 3.00; Instrument stabilization delay (s) : 15; Sample uptake delay (s) : 50; Pump rate (rpm) : 15; Rinse time (s) : 30. All the samples were digested in aqua regia and finally analysed for [Au] and [Ga] content. Commercially available reference standards for both gold and gallium were used. After every two samples, blank and reference standards were recorded for maximizing accuracy. Gold and Gallium was recorded at 242.794, 267.594 and 294.363, 417.204 nm respectively.

NMR Experiments: ^{71}Ga NMR spectroscopic analysis was performed on Bruker DRX 300MHz spectrometer using $Ga(NO_3)_3$ as an internal standard. All samples were recorded in D_2O.

XPS Spectroscopy: X-ray photoelectron spectroscopy was performed using a Kratos Axis HSi XPS instrument. Samples were dried onto the silicon wafer pieces and measured at a 90^o take-off-angle (TOA) yielding a sampling depth of ~10nm. The analysis area was ~500µm diameter. Analyses were performed with a monochromatic Al k* X-ray source powered at 15kV and 15mA. Charge neutralization of the sample surface was achieved with the use of a low-energy electron flood gun. The quantification method assumes that the sampling volume is homogeneous. High-energy solution XPS analyses of the Au4f, Ga2p, C1s, S2p, O1s and N1s regions were performed on the sample.

Cell Culture

PC-3 prostate cancer cells were obtained from the American Type Culture Collection (ATCC). PC-3 cells were maintained in RPMI medium (obtained from Gibco BRL, Grand Island, NY) supplemented with 4.5 g/L D-glucose, 25 mM Hepes, 0.11 g/L sodium pyruvate, 1.5 g/L sodiumbicarbonate, 2 mM L-glutamine, 10% FBS (Hyclone), and antibiotics.

2. Synthesis

*Synthesis of [AuNP-(DTDTPA)(Ga)] (**2**)*

Aqueous solution of $Ga(NO_3)_3$ (58 mM) was mixed with **1** (11.36mM of [Au]) dissolved in 0.01 M NaOH at room temperature with continuous stirring. Immediate precipitate formation was observed. The reaction mixture was allowed to stir for 3 hours and subsequently washed with DI water (three times) and centrifuged at 20000 rcf for 20 mins at 25ºC.

ICP analysis

To a solution of **1 (**11.36mM of [Au]) dissolved in 0.01M NaOH, a solution of increasing amounts of $Ga(NO_3)_3$ (3.9, 9.7, 19.5, 39, 58, 78, 117, 156 mM) in DI water was added. The chelated product was isolated by processing the steps as mentioned above. 1 mg/ml of the dried pellet (dissolved in 0.01M NaOH) and respective supernatants were used for ICP analysis. All measurements were performed in triplicates. To evaluate concentration of Ga that are irreversibly

chelated to **1**, we determined the concentrations of [Ga] and [Au] in **2.** Based on ICP-OES analysis, it is evident that Au/Ga ratio remains constant beyond 58 mM concentration of [Ga] (**ESI-Figure 1**).

^{71}Ga NMR spectroscopy

For titration using ^{71}Ga NMR spectroscopy, four different standard solutions of $Ga(NO_3)_3$ with the respective concentrations, 0.1M, 0.01M, 0.001M and 0.0001M, were prepared in D_2O. ^{71}Ga NMR was recorded for each of these standard solutions and peak integration values were noted. It is well-known that ^{71}Ga NMR strongly depends on the symmetry of the complex.[3] If the gallium containing complex lacks symmetry, the NMR signal disappears. In our experiment, various concentrations of $Ga(NO_3)_3$ (29.3 mM; 58.6 mM or 117 mM) were added to aqueous solutions of **1** (5 mg/mL). After stirring for 3 hours, the reaction mixtures were centrifuged (20,000 rcf, 20 min, 25°C) and the supernatants decanted and concentrated to 1 mL volume. Supernatant solutions were analyzed and peak integration values were used to calculate the amount of gallium present [Peak integration and concentrations of [Ga] were standardized by a separate experiment (**see ESI-Figure 2 and 3**)]. The slope of the graph correspond to the amount of gallium that can be coordinated to **1** (5 mg). By this NMR experiment, it is clear that 11.36 mM of [Au] in **1** requires at least 58 mM of [Ga].

*Synthesis of [AuNP(DTDTPA)(Ga)(HRP)] (**3**)*

Two different conjugates of **2** differing in gallium ion concentrations were used in our experiment. The gallium chelated gold nanoparticles, **2** ([Au] = 11.36 mM and [Ga] = 29.32 mM and 58.0 mM), were suspended in 1X PBS. To 500µl of **2**, 28 µg of 1-Ethyl-3-[3-dimethylaminopropyl]carbodiimide hydrochloride (EDC) was added in 0.1 M 2-(N-morpholino)ethane sulfonic acid (MES) buffer (pH 4.6). The reaction was stirred for 10 min at room temperature. After 10 minutes, HRP solution (0.454 M) was added to the reaction mixture in 200 µl of 0.1M MES buffer (pH 4.6) and incubated for 4 hours at room temperature with continuous stirring. Reaction mixture was centrifuged at 13500 rcf for 10 minutes at 25°C and the pellet was subsequently washed twice with 1X PBS and suspended in 1X PBS solution. Both the pellets and supernatants were used for perxoidase activity assay. The serial increase in absorption of nanoparticles (**2**)-HRP conjugate was monitored and correlated to the binding of HRP protein to **2**. The plot of absorbance vs concentration of **2** for the binding study was plotted, and the ELISA plate map is shown in **ESI-Figure 4**. The outer layer carboxylates in **2** were activated using EDC in an activation buffer and conjugated with HRP. The conjugate was

characterized by peroxidase assay using ELISA (**ESI Figure 4**) and also by measuring zeta potential, size, TEM and TEM with EDX (**ESI Figure 5**) analysis.

Peroxidase activity assay using ELISA

In a 96-well plate, 100 µl of **3** was added in the first row and serial 10 fold dilutions of the samples were made along each column using 1X PBS. To all the wells was added 50 µL of TMB (3, 3', 5, 5'-Tetra Methyl Benzidine) and one component of substrate was added. The plate was incubated at room temperature for 5 minutes and further the activity of the enzyme was stopped by addition of 50 µL of 1M HCl. The absorbance of the individual wells was recorded on a microplate reader at 450nm immediately. The ELISA studies were representative measurements from triplicates, and the readings were plotted as a graph of ng of particles versus absorbance. HRP was used traditionally as a labeling agent for C-terminal of various proteins, and presence of HRP was analyzed via coupled enzyme assays.[4,5,6,7]

3. *In Vitro* Stability

In vitro stability studies were performed by incubating solutions of **1** and **2** at various pH conditions: 2, 5, 7, 10 and 12 for the period of 24 hours. The stability behavior for both were also monitored by challenging aqueous solutions of **1** and **2** (0.5 mL) with 0.5 mL each of 0.2M cysteine, 0.2M histidine, 0.2M HSA and 10% saline solutions. The stability was measured by monitoring the UV-visible absorbance, hydrodynamic radius and zeta potential measurements at 0 hour to 96 hours (0, 1, 24, 48, 72, and 96 hours). A negligible change in UV-Vis plasmon band of **1** and **2** confirmed the retention of nanoparticulate composition with stable behavior in all the challenging solutions except cysteine.(**ESI Figure-6**) The treated solutions did not show any noticeable change in hydrodynamic radii, thus confirming the stability of these conjugates.

4. *In Vitro* Cytotoxicity

In vitro cytotoxicity evaluation of **1, 2,** DTDTPA-Ga and $Ga(NO_3)_3$ was performed as described by the supplier. (**ESI-Figure 7**) Briefly, 1 x 10^5 ml^{-1} cells at the exponential growth phase were placed in a flat bottom 96-well polystyrene-coated plate and were incubated for 12 hour in a CO_2 incubator at 5% CO_2 and 37 °C. A series of concentrations ranging from 0 to 40µg/mL (0, 1, 2.5, 5, 10, 20 and 40 µg/mL) of all samples were prepared in the medium. Each concentration was added to the plate in quadruplets. After 24 hour incubation, 10 µL per well MTT (stock solution 5 mg mL−1 PBS) (ATCC, USA) was added and kept for 4 hours, and the formazan crystals so formed were dissolved in 100 µL detergent/solubilizing buffer. The plates were kept for 2 hours

in dark at 25°C to dissolve all crystals, and the intensity of developed color was measured by micro plate reader (Epoch, BioTek, USA) operating at 570 nm wavelength. Wells with complete medium, nanoparticles, and MTT, but without cells, were used as blanks. Untreated cells were considered 100% viable.

5. Characterization of [AuNP(DTDTPA)] (1) and [AuNP(DTDTPA)(Ga)] (2)

Characterization of 1: Earlier reports predicted that **1** consist of multilayers of DTDTPA attached to AuNP surface.[1, 2] DTDTPA forms inter- and intra-layer disulfide bonds on the AuNPs. This arrangement of inter and intralayer disulfide bonds make multilayered organic shell of penta-acetic acid molecules on the surface of AuNP.[1, 2] The core size of **1** that showed hydrodynamic diameter of 88 nm as observed by DLS measurements (**ESI-Figure 10(a)**) was 2-3 nm as observed from TEM image (**ESI-Figure 10(b))**. This validates the preservation of multi-layered structure of DTDTPA on AuNP surface. Any disturbance to H-bonding network would result in destabilization of DTDTPA structural motif and these disturbances would arise from pH variations and dilutions. The changes in hydrodynamic diameter and zeta potential due to pH and dilutions have been monitored by DLS measurements.

Effect of pH: The experiment was performed on the pH range from 2 – 13. A strong dependence of size with pH variation was observed (**ESI–Table 1**). At lower pH (pH 2) the size was 2417 nm. This hydrodynamic size increase is attributed to the protonation of -COOH groups at low pH resulting in aggregation of nanoparticles. At pH 4, a decrease in size to ~213 nm was observed due to decreased protonation. However, within a pH range of 6-13, the hydrodynamic diameters of **1** remains constant at 78±4 nm (**ESI-Figure 10**) ensuring that the layered structure is intact and stable in this pH range.

Effect of dilution: We also studied the effect of dilution on the layered structure of **1** using DLS (**ESI-Table 2**). Increasing the concentrations of **1** from 0.3 mg/mL (Au = 0.05 mM) to 5 mg/mL (Au = 11.36 mM) in DI water at pH 8-8.5, no change in hydrodynamic size (average particle size = 88±4 nm) or zeta potential (average zeta potential = -72 mV) was observed.

Characterization of 2: To understand the effect of Ga chelation on the layered structure, we performed a detailed DLS study using the Ga chelated conjugate **2** in pH 8 (**ESI-Figure 11**). It is expected that if some of the carboxylate anions in **1** will complex with Ga^{3+} ions and the resultant negative charge will be relatively less than the parent construct. The zeta potential of **2** is -55mV (-81 mV for **1**) and the difference is ~25mV, suggesting the presence of free carboxylic groups and also confirming the layered structure even after chelation. The TEM images of **2** also clearly indicated that the nanoparticles are arranged in a cluster of several nanoparticles **(ESI-Figure 13**

and **ESI-Figure 14)**. It is expected that a cluster of 50-60 nanoparticles interact through macromolecular H-bonding. Such H-bonding network between nanoparticulate structures is not unusual. Further, as Ga ions surround AuNP, another layer of carboxylate is available to form conjugation with biomolecule.[8, 9] This data confirms that the structural integrity of multilayer carboxylates present in the parent **1** is retained.

Nanoparticle Tracking Analysis: Nanoparticle Tracking Analysis was also performed on both **1** and **2** to confirm the structural integrity by tracking nanoparticles simultaneously moving under Brownian motion using **(ESI-Figure 9)**. The average particle size by NTA confirmed hydrodynamic diameter of ~85 nm for **1** and no major change in size was observed for conjugate **2** (~98 nm) confirming that the structural integrity is preserved upon chelation.

6. Investigation of Ga^{3+} binding on AuNPs:

Experimental Design: Systematic experiments have been performed to confirm the chelation of Gallium atoms with DTDTPA and not present on the surface of AuNPs (**ESI-Scheme-1**). To understand whether the gold nanoparticle surface has affinity towards Ga^{3+} ions, two different "model" gold nanoparticles were chosen. Experimental results with detailed analytical data are presented below.

(i) The first model AuNP that we chose was AuNP coated with thiolated PEG-750 (AuNP-PEG-750), where in, the charge (zeta potential) of AuNP (ζ = -49 mV) is similar to that of AuNP(DTDTPA) (ζ = -81 mV) but doesn't contain any chelating ligand like DTDTPA on the surface. AuNP-PEG-750 (characterized independently) was treated with different ratios of Ga^{3+}. The reactions were performed under identical conditions as followed for the preparation of **2**. The nanoconstructs obtained were characterized by HR-TEM, EDX, UV-Visible, size and zeta analysis and the data was compared with **2**.

(ii) The second model was AuNP coated with thioctic acid (AuNP-TA). The rationale for choosing (AuNP-TA) is as follows: (a) TA group has carboxylates outside –however, it lacks chelating ligand structures as present in DTPA. (b) TA also has size (core size 3- 5nm) similarity to that of AuNP(DTDTPA) (**1**). (c) Additionally the synthetic route for preparation of TA-AuNP is also similar to those of AuNP(DTDTPA). The reaction of Ga^{3+} with TA-AuNP was performed under identical conditions as followed for the preparation of **2**. Final product was thoroughly characterized by HR-TEM, EDX, UV-Visible, size and zeta analysis and data was compared with those of **2**.

Experimental details: Reaction of AuNP-PEG with $Ga(NO_3)_3$-(**AuNP-PEG+Ga**): $Ga(NO_3)_3$ dissolved in water was added to AuNP-PEG (10.05μM [Au]) in different molar ratios (Au:Ga ratio; 1:5, 1:2.5, 1:1.125) and stirred for 3 hours at room temperature. Gold mirror formation was observed on the walls (**ESI-Figure 17**) within 5 minutes of gallium nitrate addition at all ratios. The solution was centrifuged (20,000 rcf for 20min) after 3 hours and pellets obtained were washed three times, re suspended in DI water and used for characterization.

*Reaction of TA-AuNP with $Ga(NO_3)_3$-(**TA-AuNP+Ga**)*: $Ga(NO_3)_3$ dissolved in water was added to TA-AuNP (6.7μM [Au]) in 1:5 (Au:Ga) molar ratio and after 30 minutes of addition, precipitate formation was observed and stirring was continued for 3 hours at room temperature. The solution was centrifuged (20,000 rcf for 20min) to obtain pellet and subsequently washed three times with DI water. The pellet obtained was resuspended in 0.01M NaOH and used for characterization.

Results:

HR-TEM: The HR-TEM images obtained for **AuNP-PEG+Ga** pellet (Au:Ga, 1:5) was not significantly different from those of AuNP-PEG except that larger size nanoparticles were observed. The formation of larger size nanoparticles resulted due to the aggregation induced by addition of $Ga(NO_3)_3$. With respect to **TA-AuNP+Ga** reaction, the final pellet did not show any change in size and distribution of the particles.

EDX Spectra: The EDX spectra of pellets obtained by addition of gallium nitrate to (**AuNP-PEG** (Au:Ga; 1:5) and (**TA-AuNP** (Au:Ga; 1:5) were recorded. Point and shoot technique was used to scan individual nanoparticles and the surrounding area. Scanning was performed additionally throughout the grid including dense nanoparticle regions (**ESI-Scheme 1**). If any gallium is adhered to the surface of gold nanoparticle, gallium signals would appear correspondingly. The absence of Ga $k\alpha$ signal at 9.25 in pellets (**AuNP-PEG+Ga** (1:5)) and (**TA-AuNP+Ga** (1:5)), clearly indicates that there is no affinity between gold nanoparticles and gallium ions.

Conclusions: The experimental results presented unambiguously validate that Ga ions do not attach on the surface of gold nanoparticles. As shown in **ESI-Figure 14**, STEM-HAADF image data and HR-TEM-EDX analysis of **2** indicates that at point O_2, which is located in between gold cores (away from the gold surface), we detect the presence of Ga as well as a high carbon and oxygen content. This is an independent proof that Ga^{3+} is chelated by DTDTPA. It is also worth to note here that literature evidences cite that direct interactions of Au and Ga are feasible only at high temperature (300-400^{o}C).[10, 11] Our analytical data for **2** and results from "model" nanoparticles confirm that Ga ions are *not* bound on the surface of gold nanoparticles.

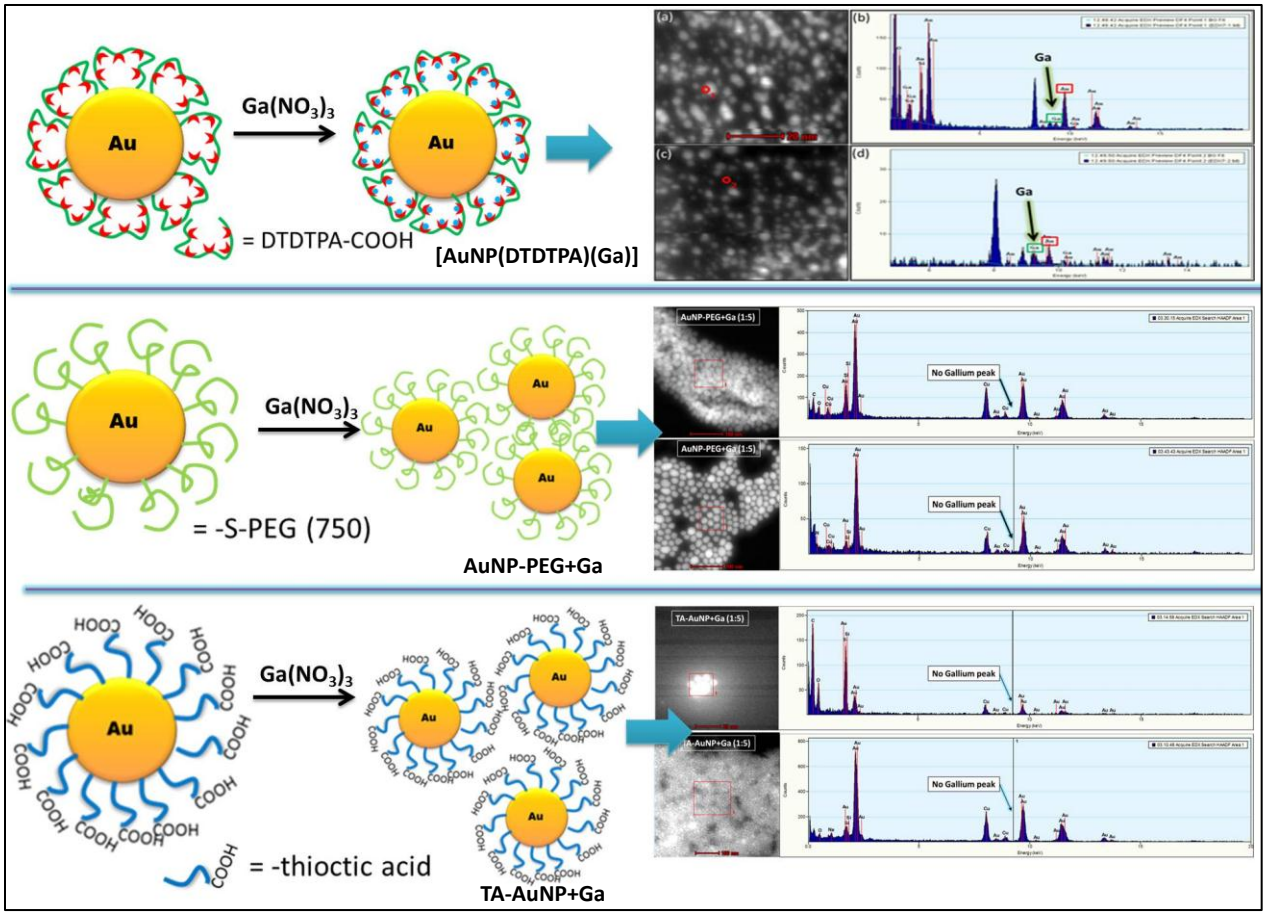

ESI-Scheme 1

Synthesis of 2, AuNP-PEG+Ga, TA-AuNP+Ga with respective HR-TEM and EDX Spectra confirming the presence and absence of Ga cations.

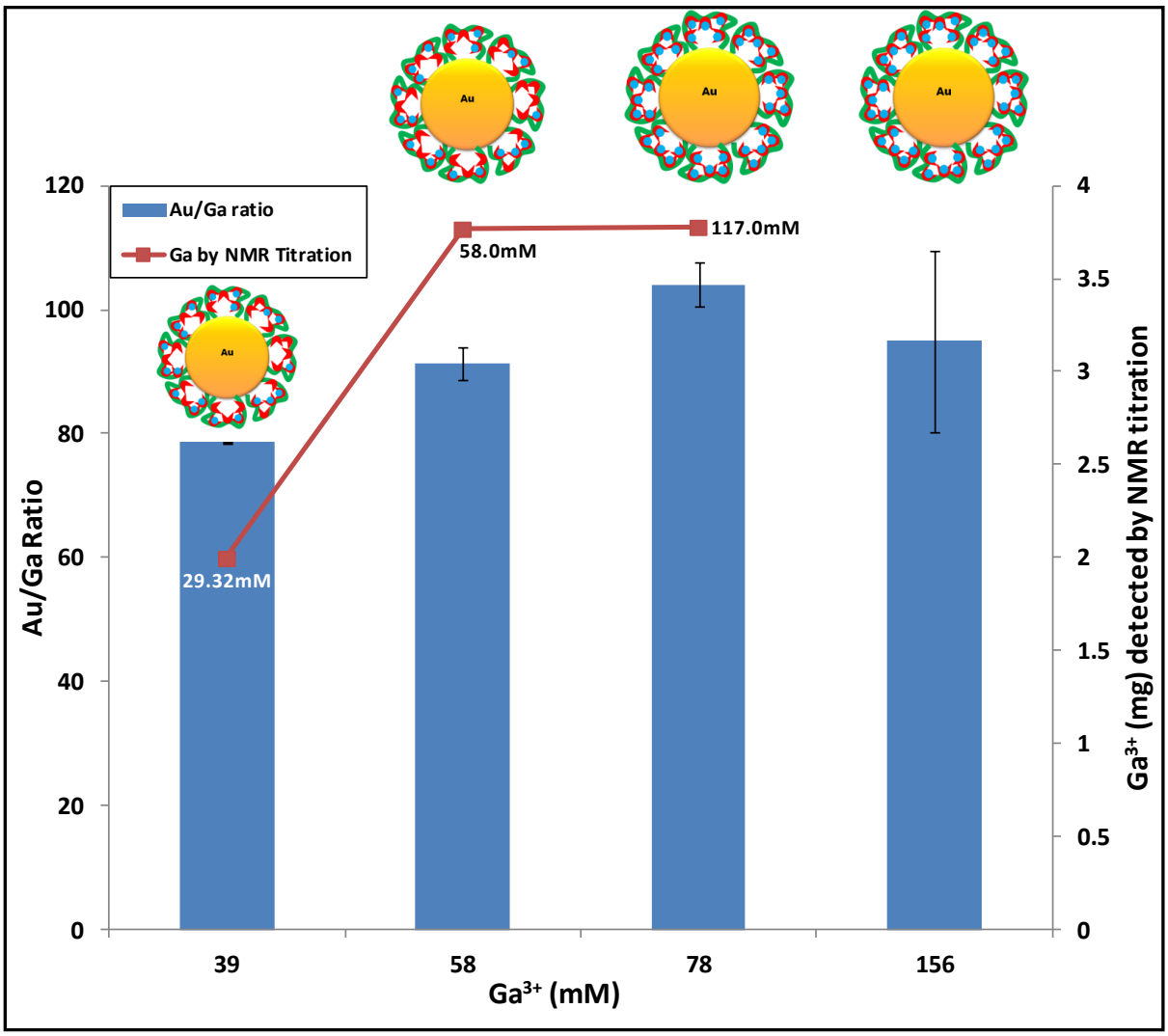

ESI-Figure 2

A graph showing titration of $Ga(NO_3)_3$ with 1 and the amount of Ga^{3+} detected by ICP-OES and ^{71}Ga-NMR in terms of Au/Ga ratio and Ga^{3+} in mg respectively.

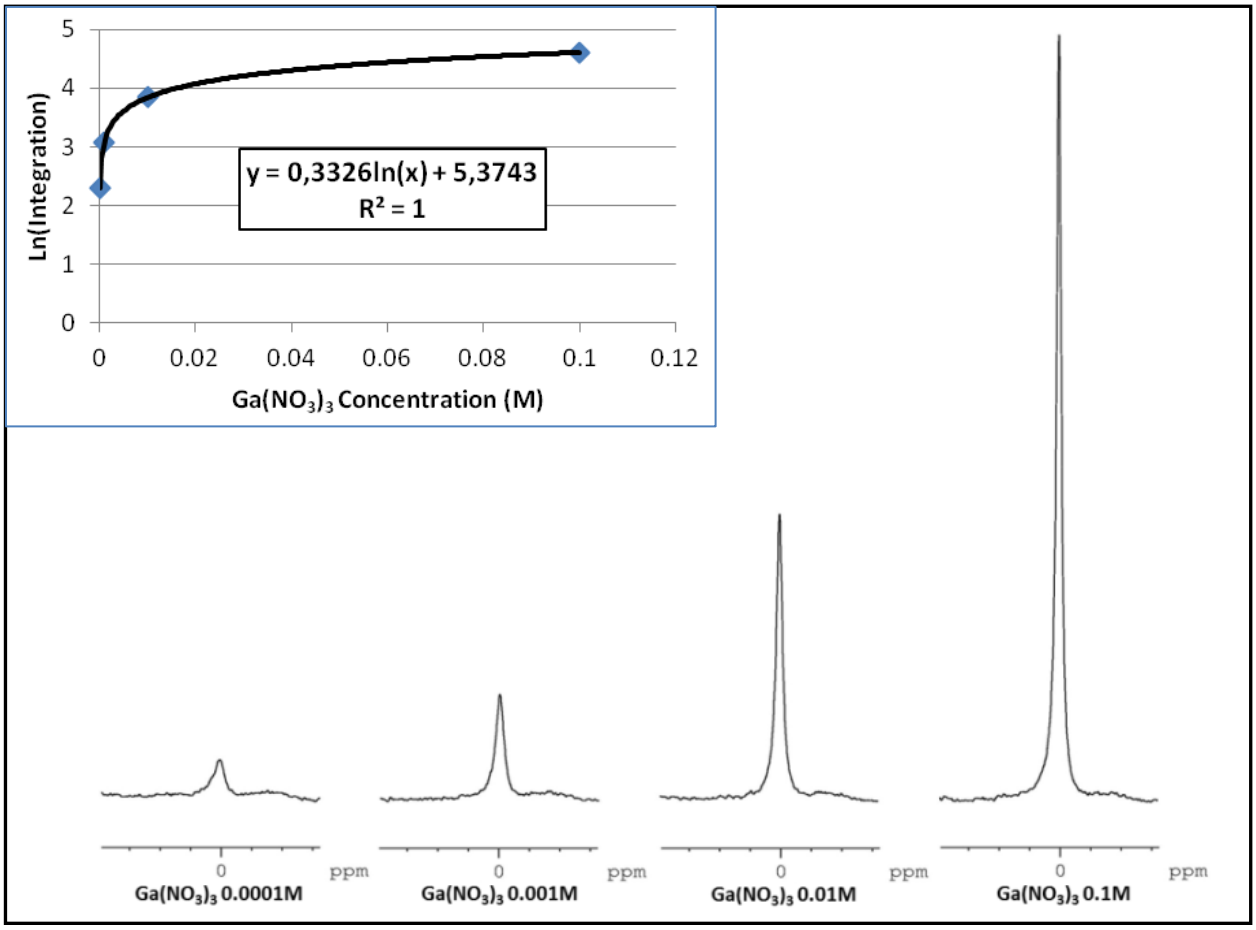

ESI-Figure 3

^{71}Ga NMR spectra of the standard solutions of $Ga(NO_3)_3$ with concentrations of 0.1M, 0.01M, 0.001M, and 0.0001M in D_2O. Through the integration of the ^{71}Ga NMR peaks a standard curve of the logarithmic integration was obtained for the different known solutions of $Ga(NO_3)_3$ as shown in *inset*. It should be noted that the integrations were done considering the integration value of 100 to the highest concentrated solution of $Ga(NO_3)_3$ (0.1M).

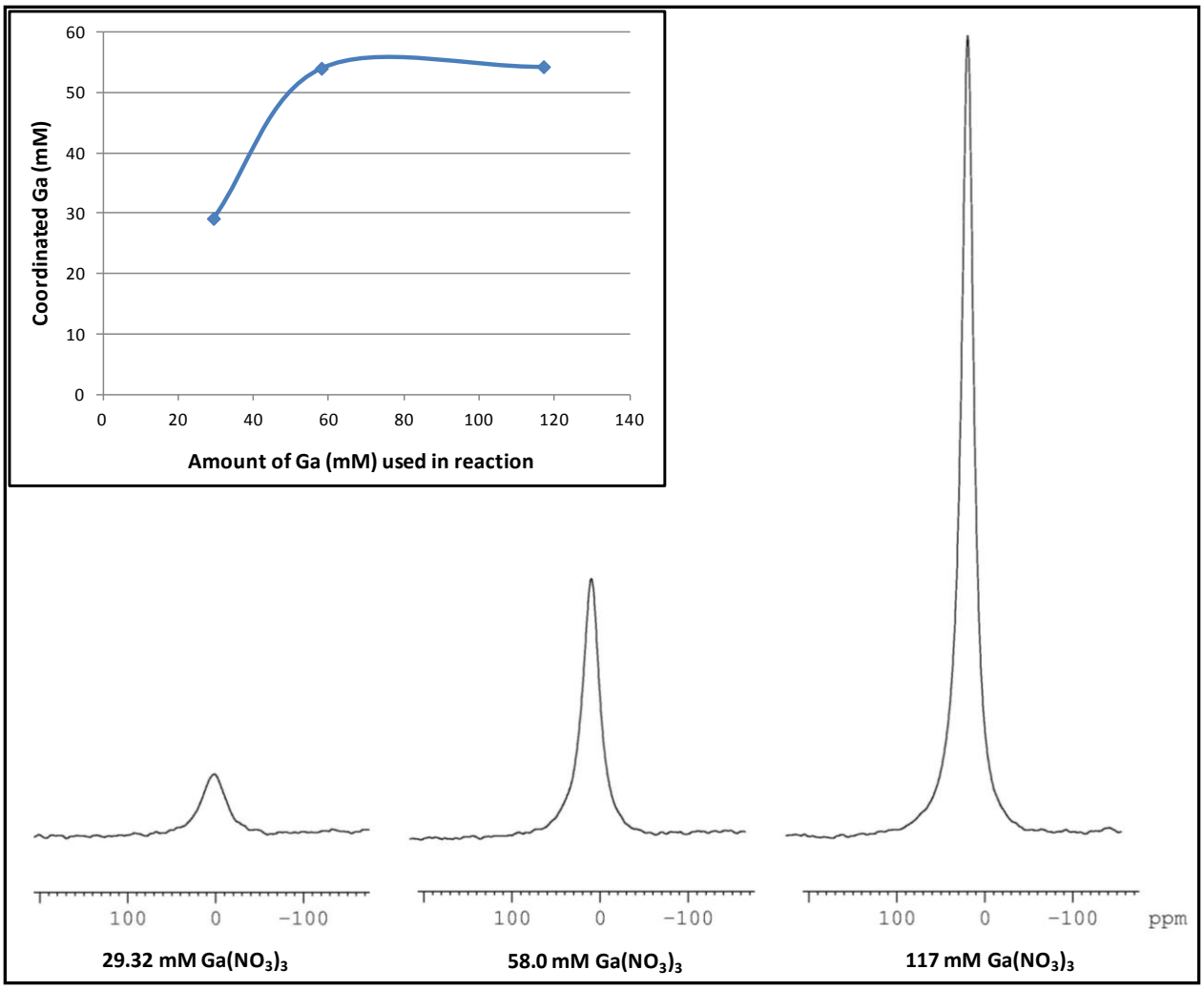

ESI-Figure 4

^{71}Ga NMR spectra of the reaction supernatants of 1 with different amounts of $Ga(NO_3)_3$. Inset shows the amount of gallium coordinated to 11.36 mM [Au] in AuNP-DTDTPA at various concentrations of $Ga(NO_3)_3$.

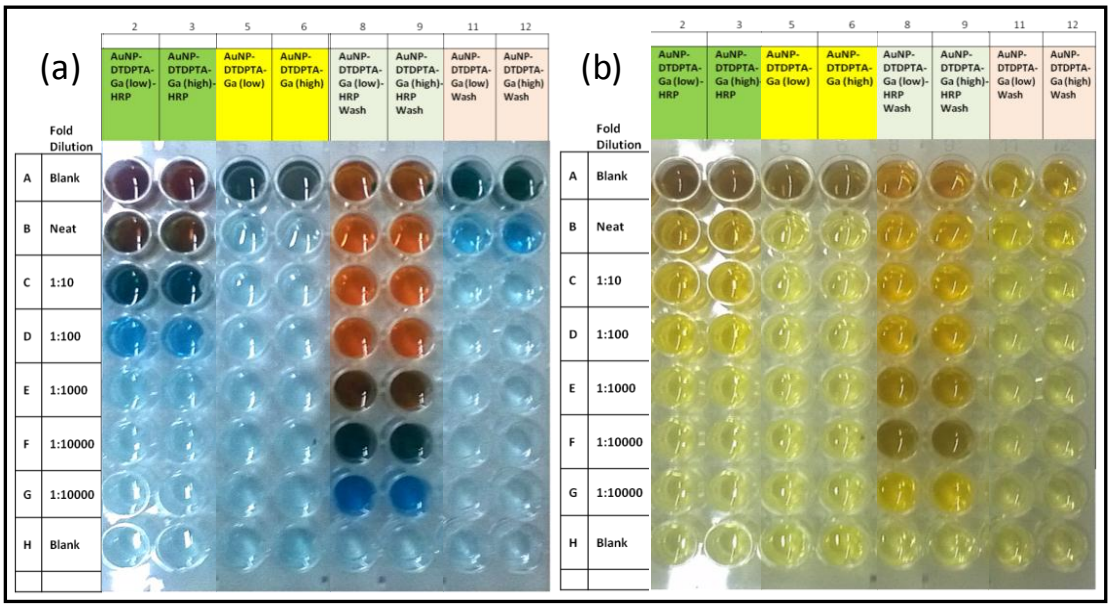

ESI-Figure 5

HRP Conjugation Assay (a) 96-well plate image after addition of substrate and (b) stop reagent.

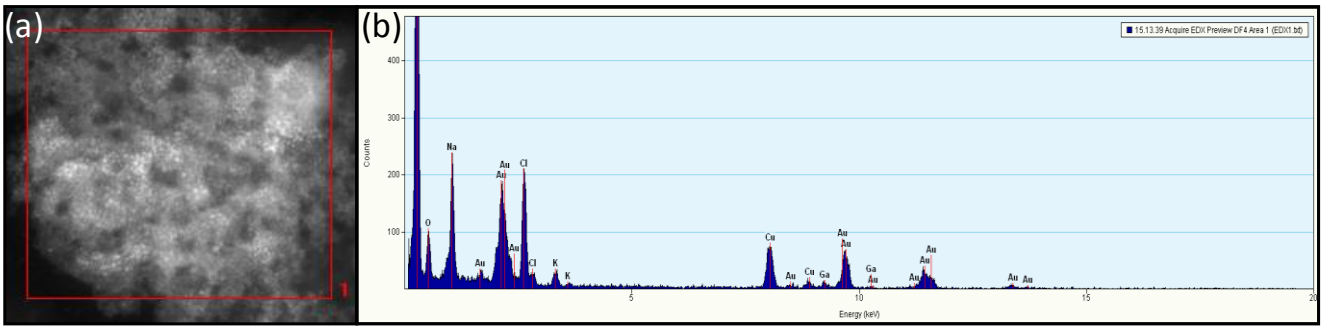

ESI-Figure 6

(a) TEM image of 3; (b) EDX spectrum from a group of nanoparticles showing the presence of gold and gallium in HRP conjugated nanoconstruct on a copper/carbon grid.

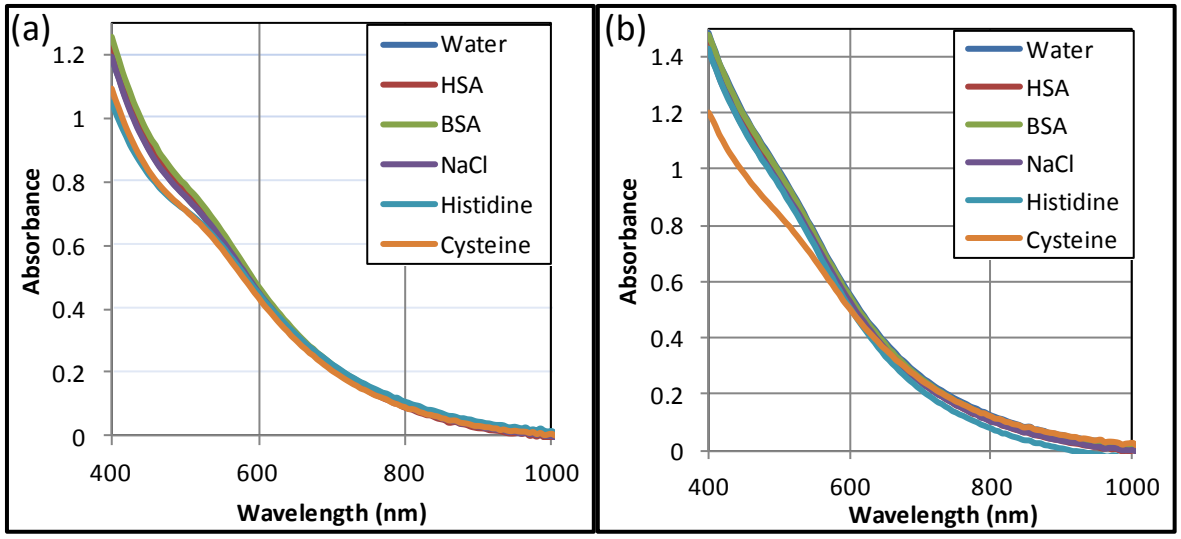

ESI-Figure 7

In Vitro **stability studies of (a) 1 and (b) 2 under various biological media of 10% NaCl, 0.5% cysteine, 0.2 M histidine, 0.5% HSA, and 0.5% BSA solutions. UV−visible absorption spectrum of these solutions after 24 hours treatment was recorded.**

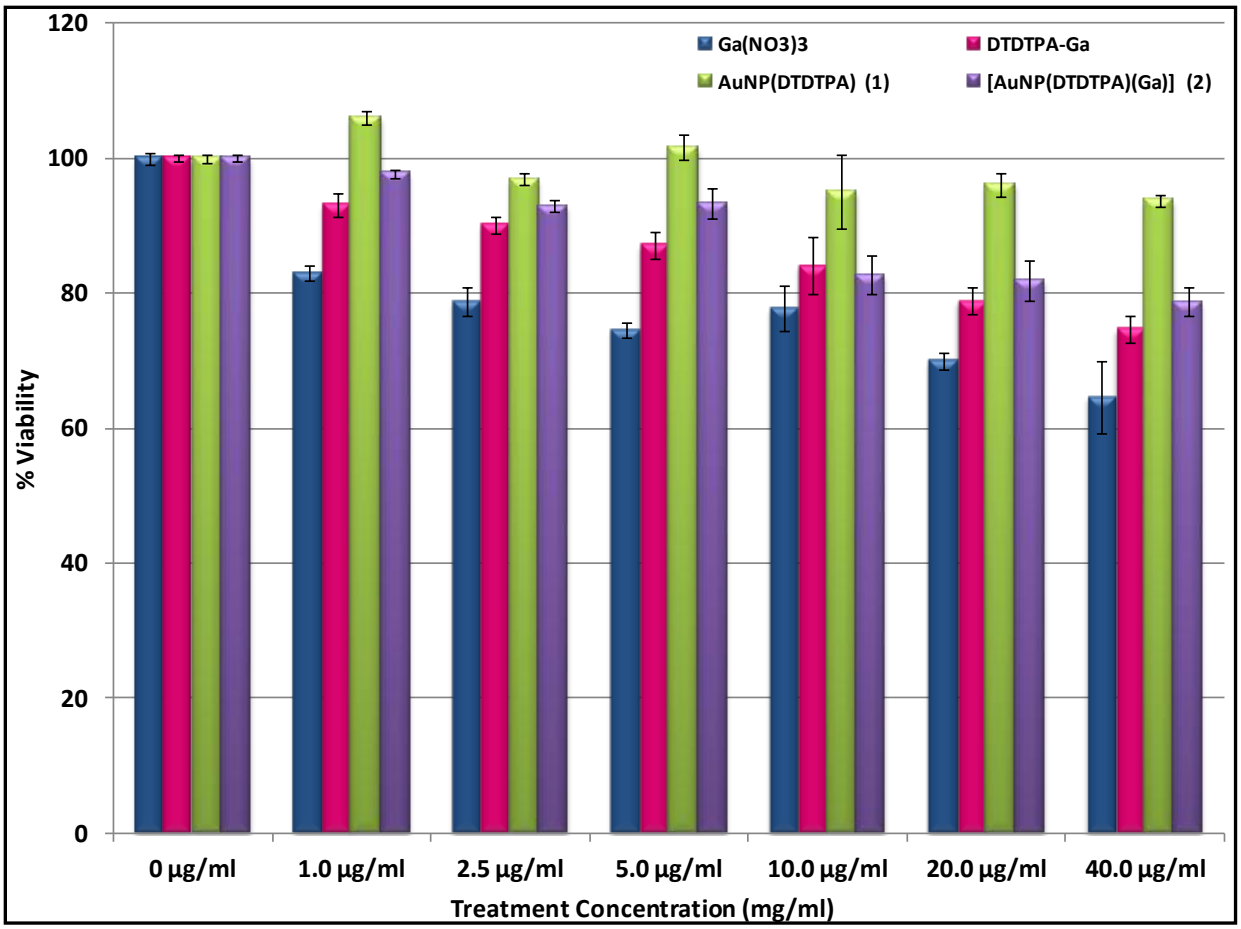

ESI-Figure 7

Cell Viability of Prostate Cancer (PC-3) cells after 24 hours incubation with increasing concentrations of 1, 2, DTDTPA-Ga, and $Ga(NO_3)_3$.

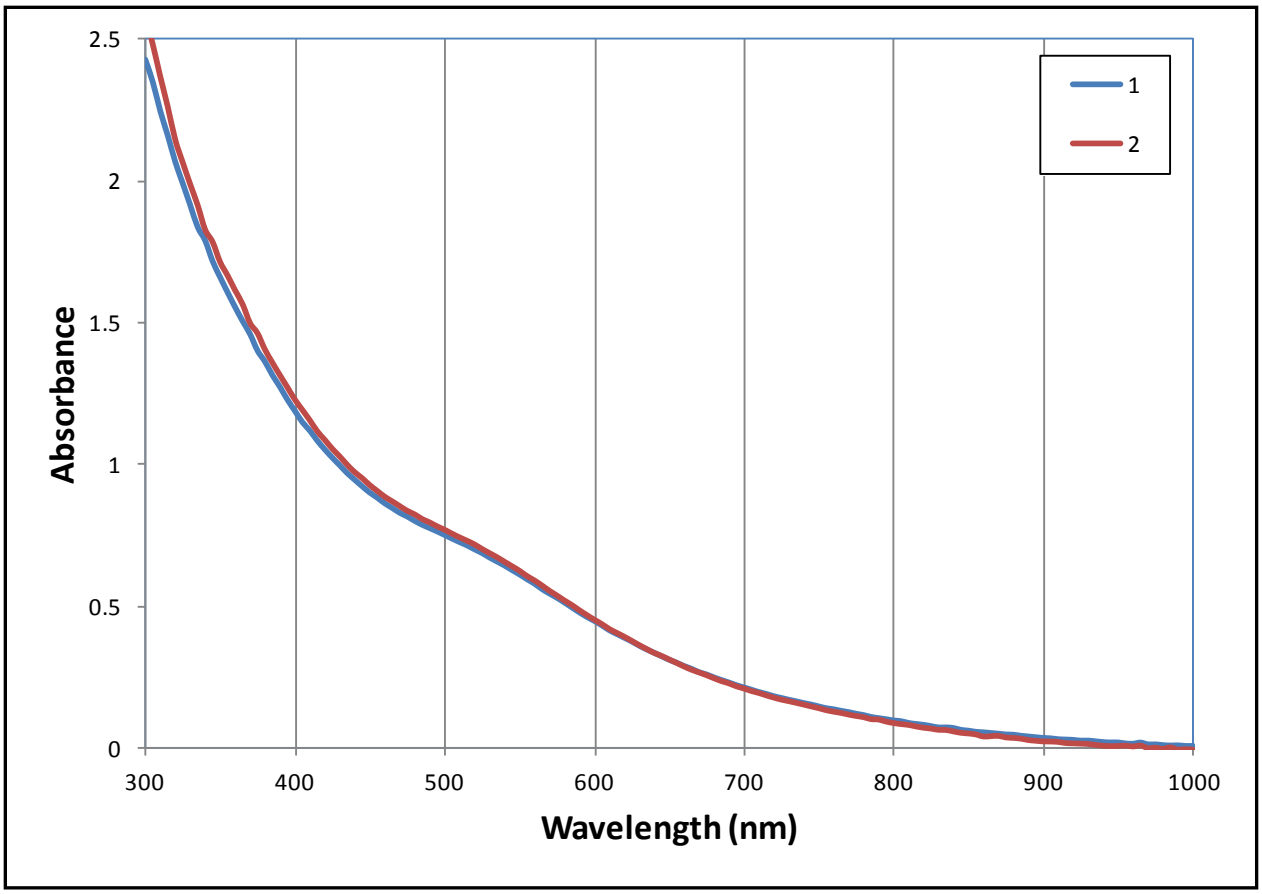

ESI-Figure 8

UV-Visible absorption spectrum of 1 and 2.

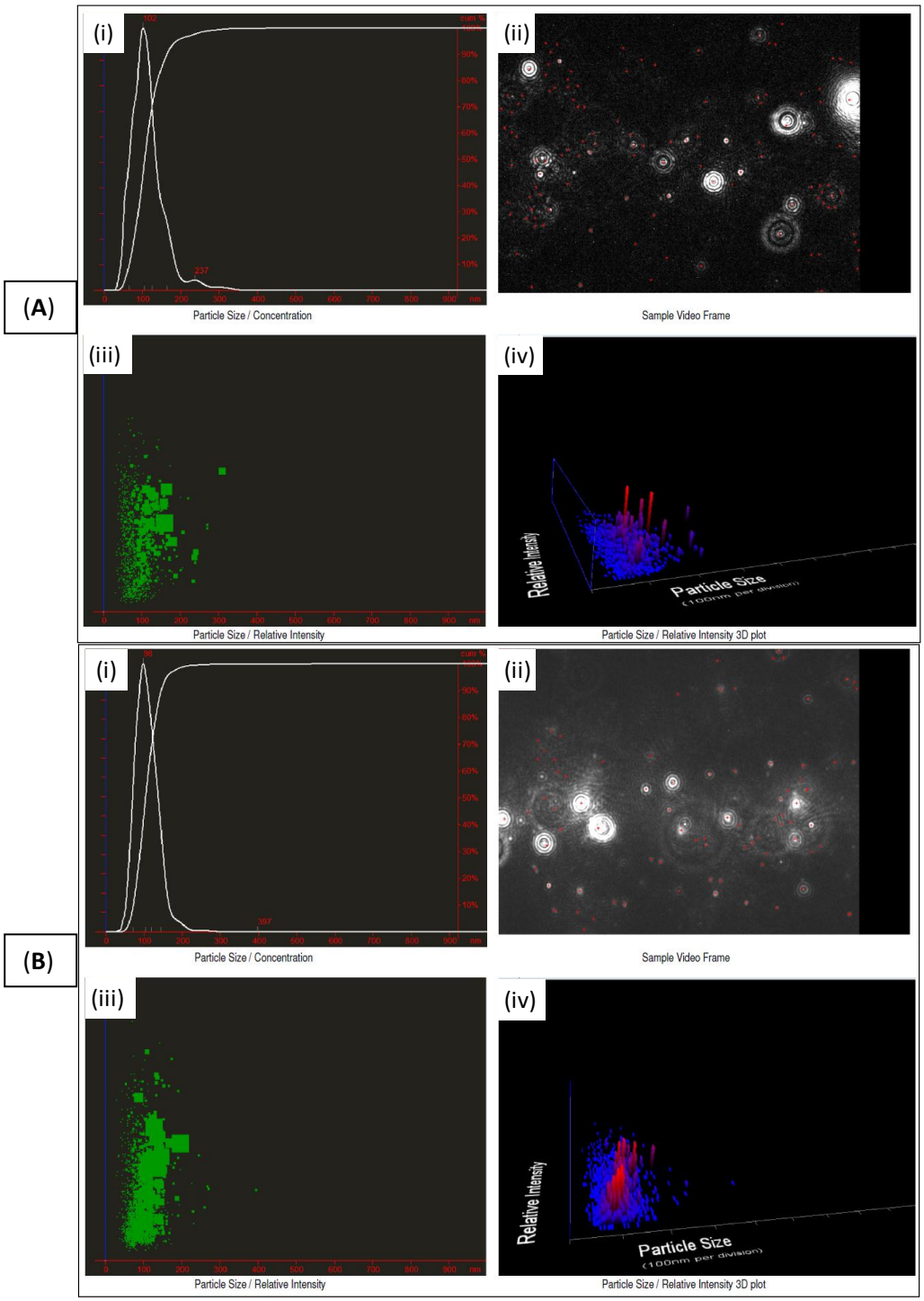

ESI-Figure 9

Nanoparticle Tracking Analysis (NTA) of 1 and 2 using NanoSight, UK. (A) (i) A size analysis plot showing the size distribution of **1** with respect to the concentration of nanoparticles corresponding to its video frame shown in (ii); (iii) A plot of size distribution of **1** as a function of scattered intensity; and (iv) 3D graph of Size Vs Intensity Vs Concentration of **1**; (B) (i) A size analysis plot showing the size distribution of **2** with respect to the concentration of nanoparticles corresponding to its video frame (ii); (iii) a plot of size distribution of **2** as a function of scattered intensity and (iv) 3D graph of Size Vs Intensity Vs Concentration of **2**.

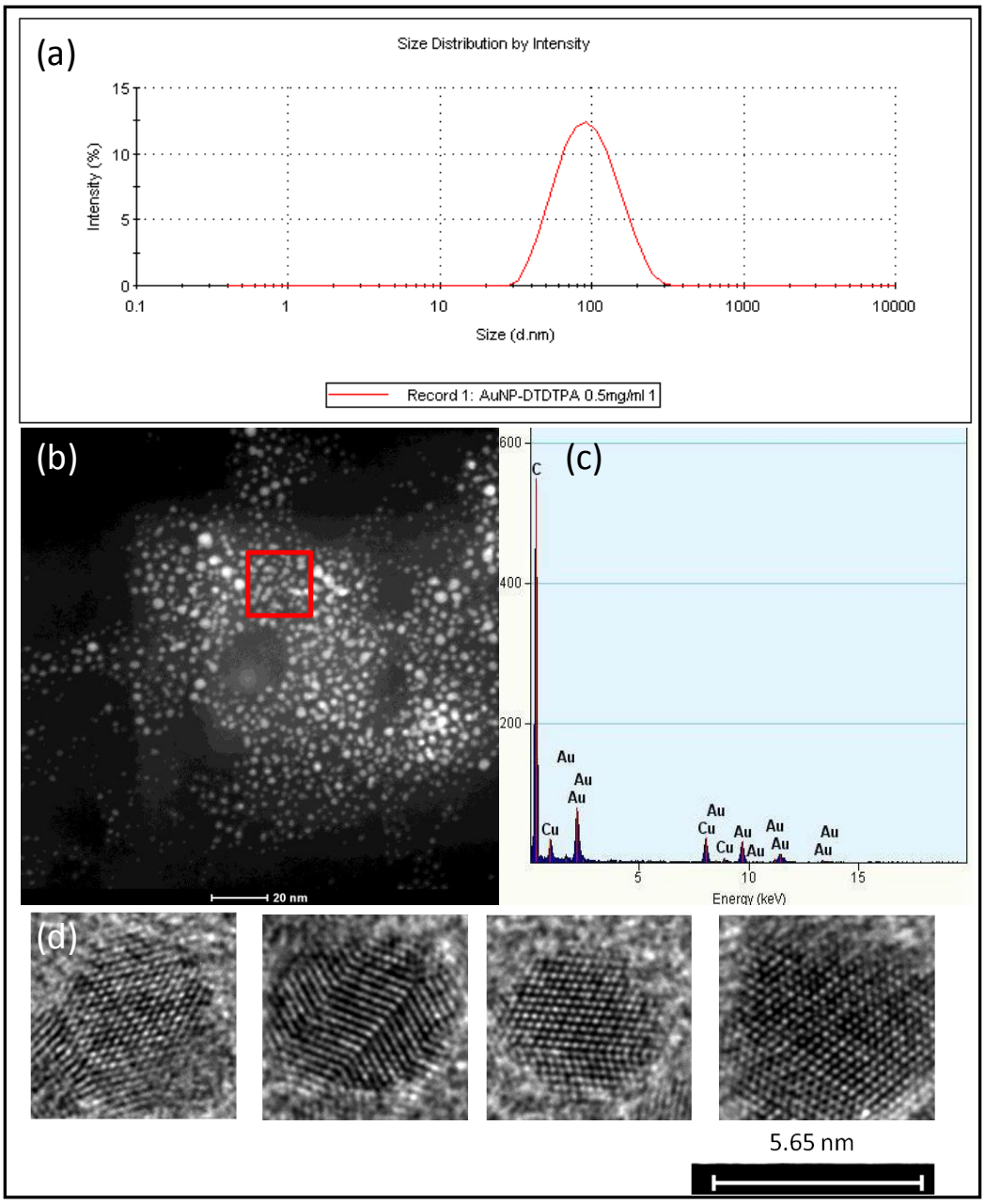

ESI-Figure 10

(a) Hydrodynamic size analysis of 1 by dynamic light scattering (DLS) performed on Zetasizer Nano S90 (Malvern Instruments Ltd. USA); (b) STEM-HAADF images of 1 with (c) EDX spectrum from a group of nanoparticles (shown by red square) showing the presence of gold in 1 on a copper/carbon grid; (d) HRTEM images of 1 showing characteristic icosahedral symmetry of AuNPs.

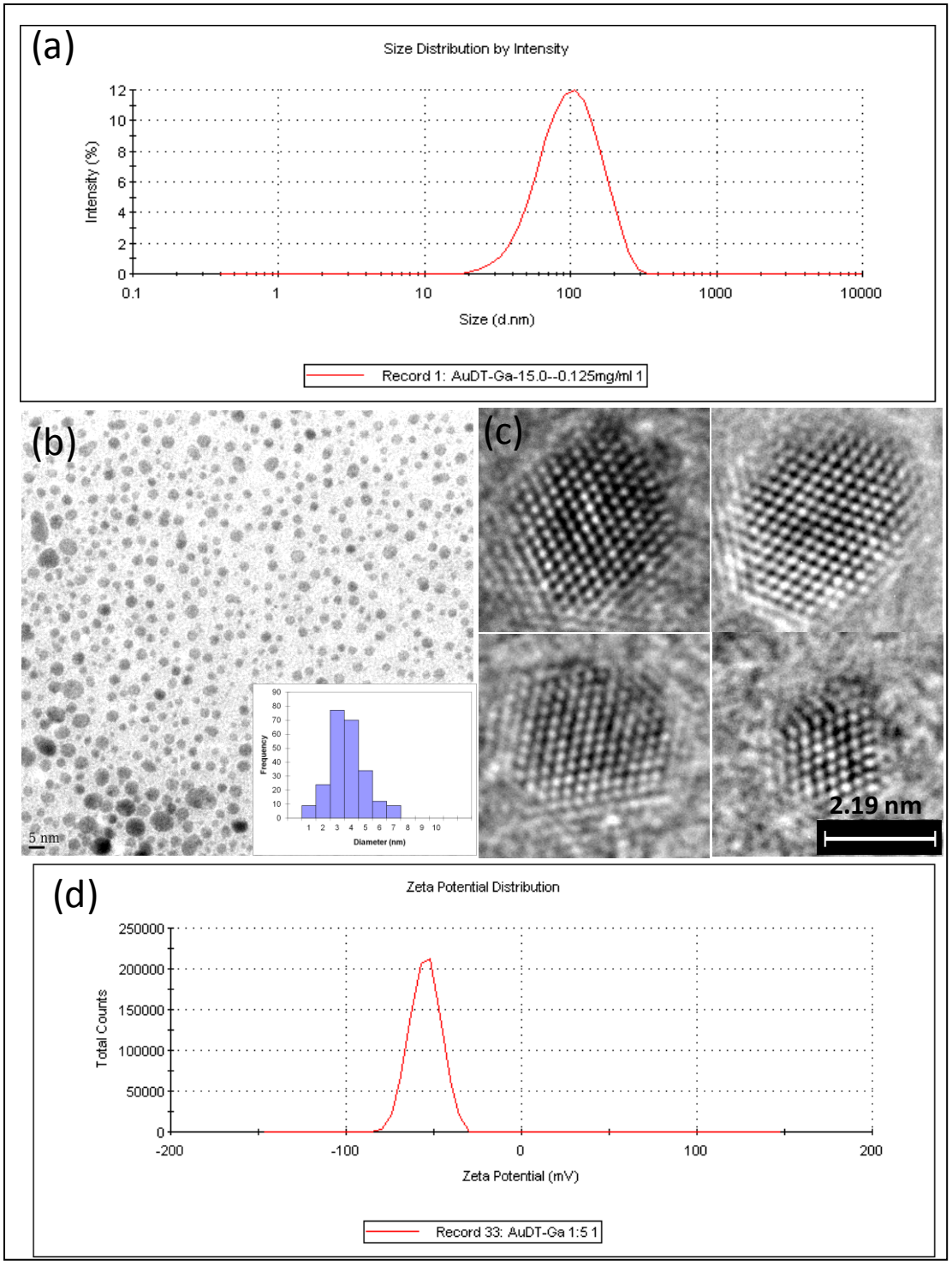

ESI-Figure 11

(a) Hydrodynamic size analysis of 2 by dynamic light scattering (DLS) performed on Zetasizer Nano S90 (Malvern Instruments Ltd. USA); (b) TEM image with histogram (*Inset*); (c) HRTEM image of immobilized solution 2 on copper/carbon grid dried overnight by acetone immersion showing characteristic icosahedral symmetry of AuNPs; (d) Zeta Potential of 2 (-55mV).

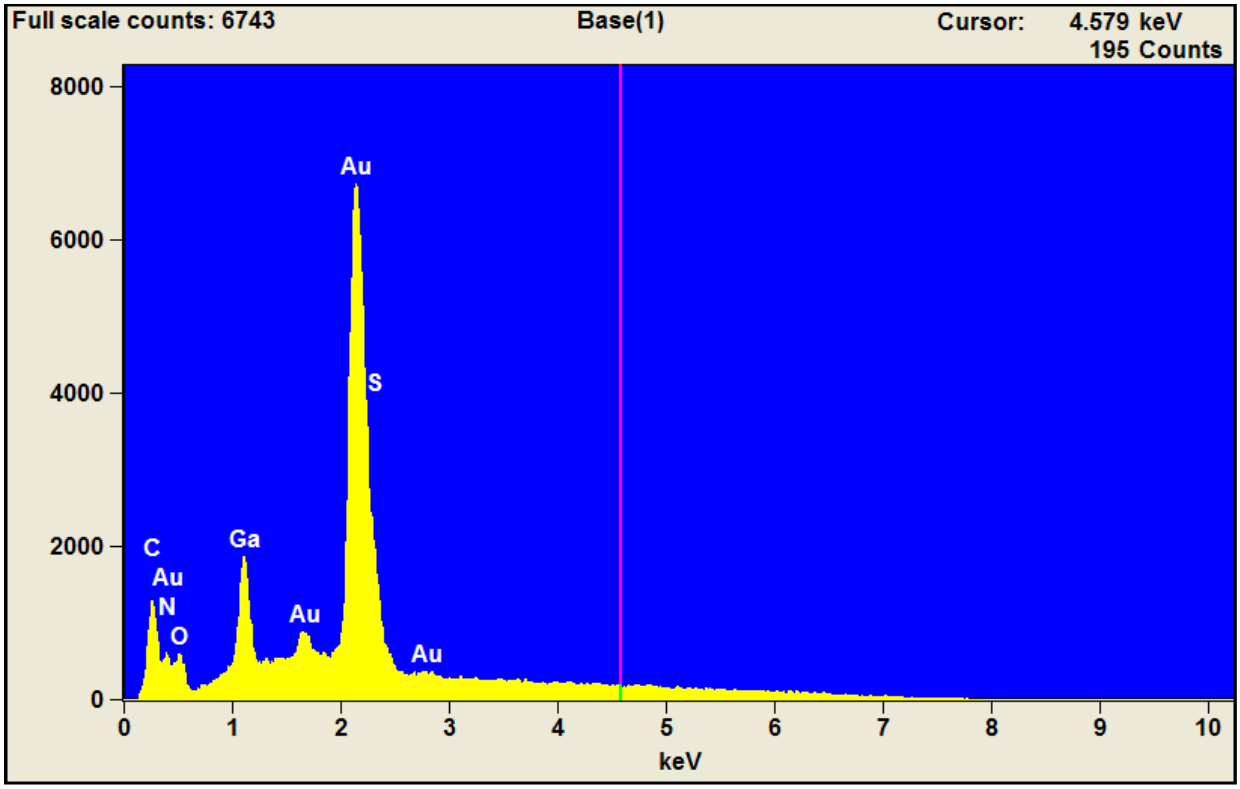

ESI-Figure 12

EDX spectrum of 2 showing presence of both Au and Ga in sample 2; the table shows the percentage of atomic concentration in 2.

Element Line	*Net Counts*	*K-Ratio*	*Weight %*	*Weight % Error*	*Norm. Wt.%*	*Atom %*	*Atom % Error*
C K	12150	0.07	11.86	+/- 0.16	11.86	37.02	+/- 0.99
N K	4979	0.05	10.16	+/- 0.41	10.16	27.20	+/- 2.19
O K	5695	0.03	6.03	+/- 0.17	6.03	14.13	+/- 0.80
S K	17790	0.07	5.77	+/- 0.18	5.77	6.74	+/- 0.43
S L	529	0.00	---	---	---	---	---
Ga K	0	0.00	---	---	---	---	---
Ga L	15758	0.07	6.63	+/- 0.09	6.63	3.56	+/- 0.10
Au L	8	0.00	---	---	---	---	---
Au M	116204	0.70	59.55	+/- 0.44	59.55	11.34	+/- 0.17
Total			100.00		100.00	100.00	

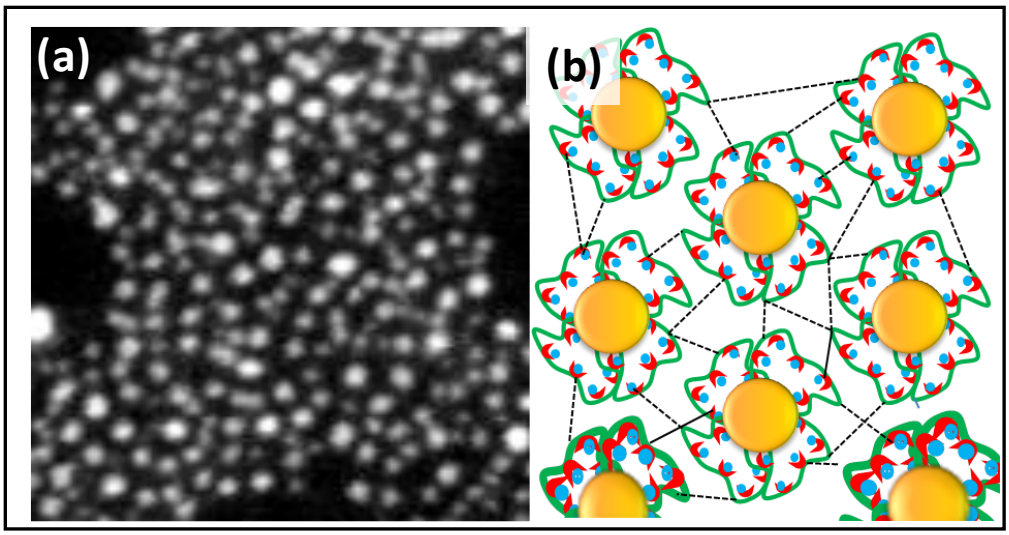

ESI-Figure 13

(a) STEM image of 2 showing the arrangement of nanoparticles in a cluster; and (b) A possible hydrogen bonding network as shown in dashed black lines.

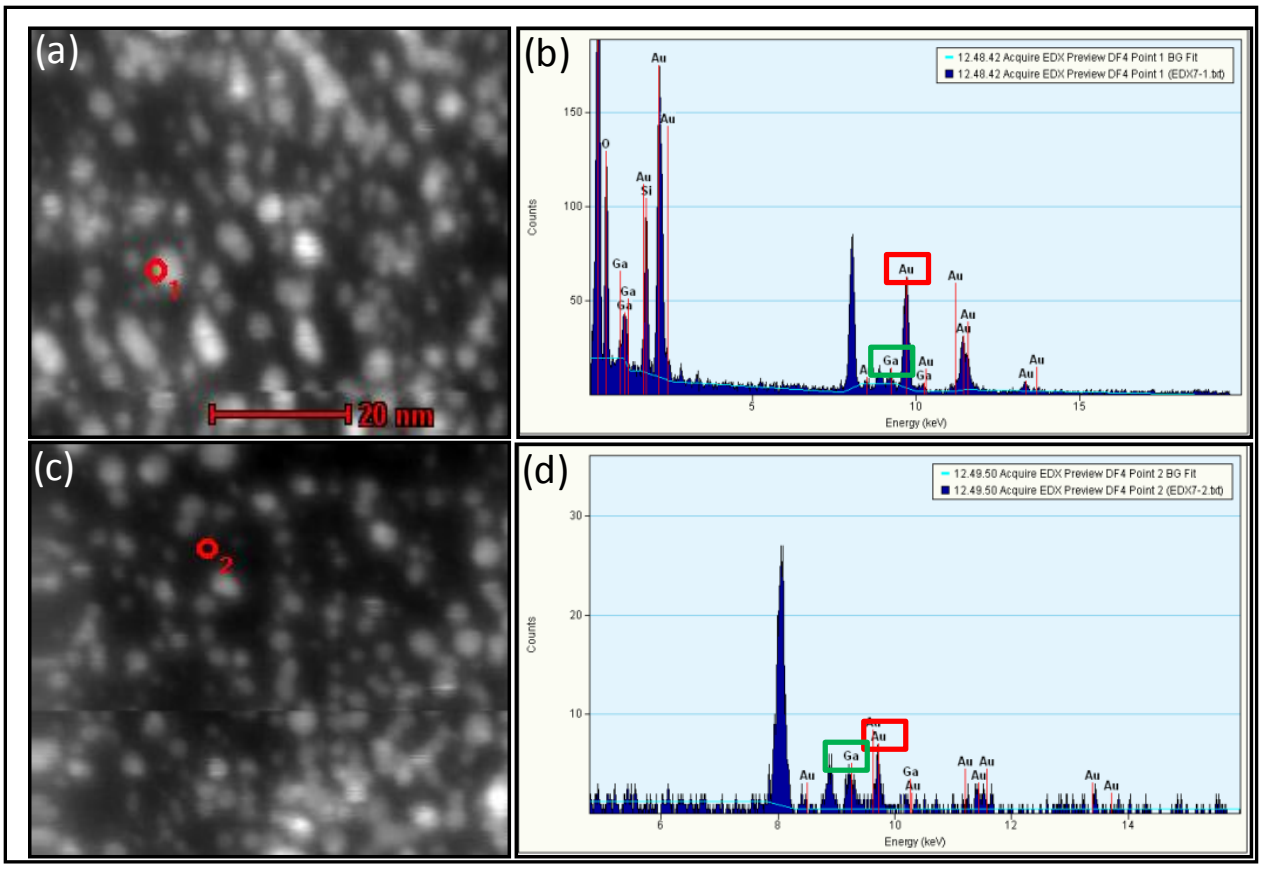

ESI-Figure 14

STEM-EDX analysis of immobilized solution of 2 with point and shoot EDX analysis on a single nanoparticle shown by O_1 (a) and the hydrodynamic area surrounded between two nanoparticles by a distance of 2 X 2 nm is shown by O_2 (c). The EDX analysis of point O_1 (b) and O_2 (d) indicate the presence of Au and Ga, the point O_1 (b) showed higher amount of Au than Ga, while in point O_2 (d) higher amount of Ga is present and Au is comparatively less. It is also important to note the high amount of carbon and oxygen present.

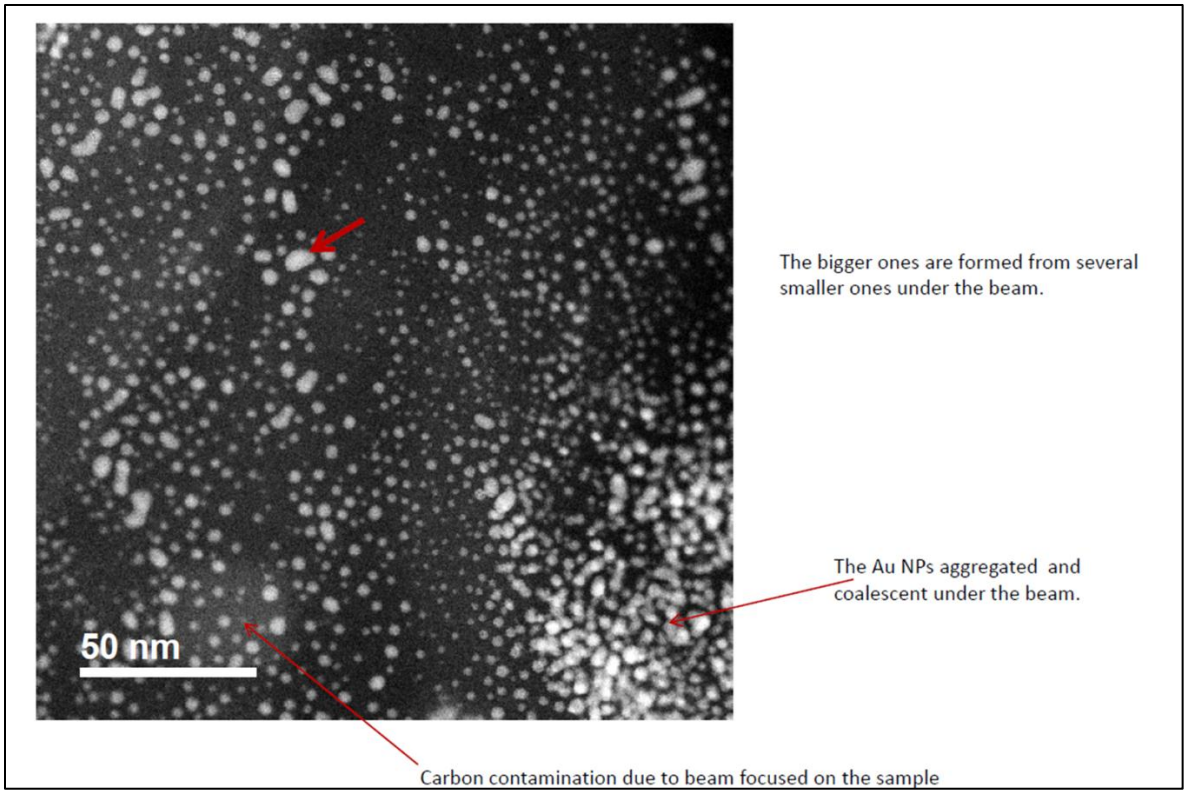

ESI-Figure 15

STEM-HAADF image showing electron beam induced aggregation of 2.

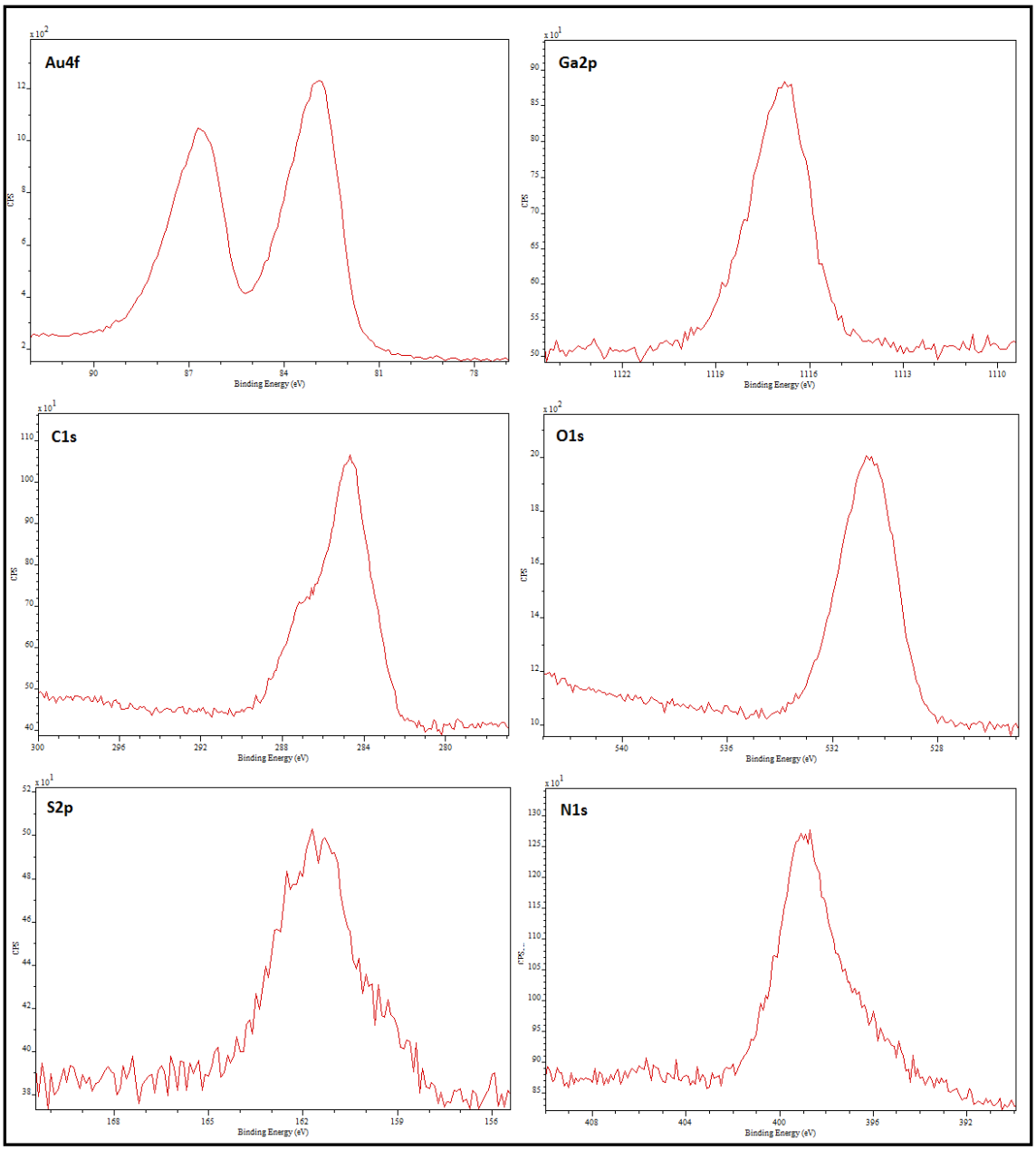

ESI-Figure 166

XPS high resolution spectra of region Au4f, Ga2p, C1s, O1s and S2p in 2. Table shows summary binding energies (eV), Atomic Mass, Percent atomic and Mass concentration measured by XPS.

Peak	Position BE (eV)	FWHM (eV)	Raw Area (CPS)	RSF	Atomic Mass	Atomic Conc. %	Mass Conc. %
Au4f	83.200	1.972	17712.8	6.250	196.967	6.48	46.44
Ga2p	1116.800	2.049	5220.0	5.581	69.725	1.88	4.78
C1s	284.800	4.319	6029.6	0.278	12.011	45.59	19.91
O1s	530.000	2.469	5614.3	0.780	15.999	13.99	8.14
S2p	160.800	3.804	2056.8	0.668	32.065	6.71	7.82
N1s	398.800	3.627	5972.6	0.477	14.007	25.34	12.91

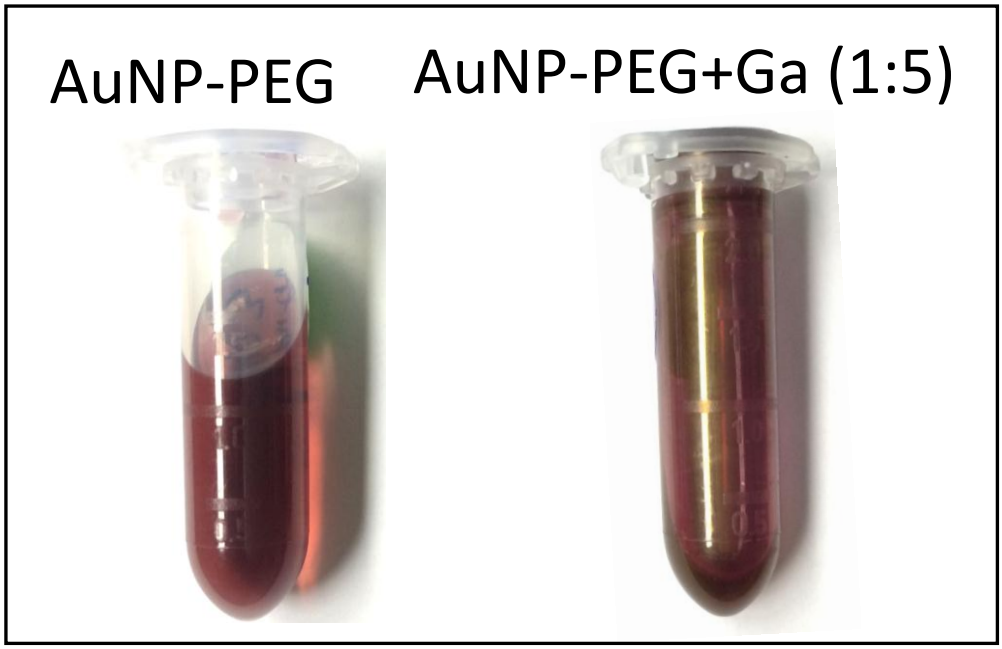

ESI-Figure 177

Gold mirror deposition after addition of $Ga(NO_3)_3$ to AuNP-PEG.

ESI-Table 1

Size analysis and Zeta potential measurements of 1 at standard pH buffer solutions

Conc. of 1 (mg/ml)	pH	Conc of Au (mM)	Size by DLS (nm)		Zeta Potential (mV)		Observations
			Mean	Std dev	Mean	Std dev	
0.50	2	1.16	2417	315	19	1.06	Suspension
0.50	4	1.16	213	1.60	-32	1.41	Partially Soluble
0.50	5	1.16	212	1.60	-40	0.28	Partially Soluble
0.50	6	1.16	76	0.39	-33	2.90	Soluble (Clear Solution)
0.50	9	1.16	82	1.00	-54	0.14	Soluble (Clear Solution)
0.50	11	1.16	78	1.17	-53	0.98	Soluble (Clear Solution)
0.50	13	1.16	74	0.62	-48	2.60	Soluble (Clear Solution)

ESI-Table 2

Size analysis and Zeta potential measurements of 1 at various dilutions

Conc. of 1 (mg/ml)	Dilution	Conc of Au (mM)	pH	Size by DLS (nm)		Zeta Potential (mV)		Size by NTA (nm)
				Mean	Std dev	Mean	Std dev	
0.03	5ul of stock	0.050	7.80	92	2.14	-70	0.78	ND
0.05	10ul of stock	0.101	8.18	88	0.16	-80	0.49	ND
0.13	25ul of stock	0.303	7.92	90	1.05	-77	0.21	77
0.25	50ul of stock	0.555	7.91	90	0.85	-79	4.73	98
0.50	100ul of stock	1.16	8.53	88	0.65	-71	0.21	63
1.00	200ul of stock	2.27	8.73	84	0.3	-68	0.49	102
1.00	200ul of stock - recorded after 24h	2.27	8.73	84	0.42	-65	2.96	ND
5.00	Stock Solution	11.36	-	126	2.08	NM	-	NM

ND: Not Determined; NM: Not Measurable

ESI-Video Clip

Video clip showing the effect of electron beam (HR-TEM) on 2.

[AuNP(DTDTPA)(Ga)] Video.wmv

References:

1. C. Alric, J. Taleb, G. Le Duc, C. Mandon, C. Billotey, A. Le Meur-Herland, T. Brochard, F. Vocanson, M. Janier, P. Perriat, S. Roux and O. Tillement, *J Am Chem Soc*, 2008, **130**, 5908-5915.
2. P.-J. Debouttière, Roux, S., Vocanson, F., Billotey, C., Beuf, O., Favre-Réguillon, A., Lin, Y., Pellet-Rostaing, S., Lamartine, R., Perriat, P. and Tillement, O., *Advanced Functional Materials*, 2006, **16**, 2330-2339.
3. Q. Zhou, C. Henoumont, L. Vander Elst, S. Laurent and R. N. Muller, *Contrast Media Mol Imaging*, 2011, **6**, 165-167.
4. N. N. Ugarova, G. D. Rozhkova and I. V. Berezin, *Biochim Biophys Acta*, 1979, **570**, 31-42.
5. G. H. Carlsson, P. Nicholls, D. Svistunenko, G. I. Berglund and J. Hajdu, *Biochemistry*, 2005, **44**, 635-642.
6. K. G. Welinder, *FEBS Lett*, 1976, **72**, 19-23.
7. N. C. Veitch, *Phytochemistry*, 2004, **65**, 249-259.
8. N. A. Kotov, *Nanoparticle assemblies and superstructures*, Dekker/CRC Press, Boca Raton, 2006.
9. R. Zirbs, F. Kienberger, P. Hinterdorfer and W. H. Binder, *Langmuir*, 2005, **21**, 8414-8421.
10. H. S. Yazdanpanah MM, Cohn RW., *Applied Physics Letters*, 2004, **85**, 1592-1594.
11. F. N. Weizer VG, *Journal of Applied Physics*, 1988, **64**, 4618-4623.